

# Analysis of the Optimal Channel Density of the Squid Giant Axon Using a Reparameterized Hodgkin–Huxley Model

Thomas D. Sangrey,<sup>1</sup> W. Otto Friesen,<sup>2</sup> and William B Levy<sup>1</sup>

<sup>1</sup>Department of Neurosurgery, University of Virginia, Charlottesville 22908; and <sup>2</sup>Department of Biology, University of Virginia, Charlottesville, Virginia 22904

Submitted 7 July 2003; accepted in final form 19 January 2004

**Sangrey, Thomas D., W. Otto Friesen, and William B Levy.** Analysis of the optimal channel density of the squid giant axon using a reparameterized Hodgkin–Huxley model. *J Neurophysiol* 91: 2541–2550, 2004; 10.1152/jn.00646.2003. A reparameterized Hodgkin–Huxley-type model is developed that improves the 1952 model's fit to the biological action potential. In addition to altering Na<sup>+</sup> inactivation and K<sup>+</sup> activation kinetics, a voltage-dependent gating-current mechanism has been added to the model. The resulting improved model fits the experimental trace nearly exactly over the rising phase, and it has a propagation velocity that is within 3% of the experimentally measured value of 21.2 m/s (at 18.5°C). Having eliminated most inaccuracies associated with the velocity-dependent rising phase of the action potential, the model is used to test Hodgkin's maximum velocity hypothesis, which asserts that channel density has evolved to maximize conduction velocity. In fact the predicted optimal channel density is more than twice as high as the actual squid channel density. When the available capacitance is reduced to approximate more modern serial Na<sup>+</sup>-channel models, the optimal channel density is 4 times the actual value. We suggest that, although Hodgkin's maximum velocity hypothesis is acceptable as a first approximation, the microscopic optimization perspective of natural selection will not explain the channel density of the squid unless other constraints are taken into account, for example, the metabolic costs of velocity.

## INTRODUCTION

A theoretical estimation of the channel density of the squid giant axon based on evolutionary arguments was first made by Hodgkin (1975). Hodgkin's velocity optimization perspective seeks to explain how the squid giant axon evolved its present channel density. Before proceeding on a renewed analysis of Hodgkin's ideas, we describe the known inaccuracies of the 1952 squid action potential model, particularly those inaccuracies relevant to a careful examination of the velocity optimization hypothesis.

### *Hodgkin's maximum velocity hypothesis*

A useful strategy for studying biology is to step into the role of nature, asking what selective changes could produce an organism that is more efficient or more likely to survive. Using a biological model that is sufficiently accurate, one can selectively tune parameters to optimize a specific quantified function of an organism according to a hypothesized design specification. A seminal and apparently successful example in neuroscience that uses this strategy is Barlow's (1952) predic-

tion for the optimal size of ommatidia versus insect eye diameter. Here we reconsider Hodgkin's proposal (1975) concerning action potential velocity and Na<sup>+</sup> channel density.

Hodgkin (1975) proposes that the squid, which uses its giant axon to control escape jetting, has evolved to maximize the action potential's propagation velocity by optimizing the Na<sup>+</sup> channel density. He points out that, on the one hand, an increased channel density produces greater current per unit length, leading to more rapid depolarization of the membrane, thus increasing the propagation velocity. On the other hand, at very high Na<sup>+</sup> channel densities the gating current, which increases in proportion to channel density, begins to limit the rate of depolarization. That is, the Na<sup>+</sup> gating charge movement acts as a transient capacitance and reduces the propagation velocity. Thus, he proposes that there is an optimum Na<sup>+</sup> channel density that maximizes conduction velocity for a given axon diameter. According to this hypothesis, the value of the channel density that maximizes the velocity should coincide with the channel densities observed in the squid giant axon.

It remains unclear whether the squid has indeed evolved to maximize conduction velocity. Hodgkin's calculations are approximate and make use of a fixed gating capacitance that is proportional to the Na<sup>+</sup> channel density. The optimum velocity, according to Hodgkin, has a relatively flat maximum centered at a channel density of 1,000 per  $\mu\text{m}^2$ , more than twice as high as the measured value of 480 per  $\mu\text{m}^2$  for the squid (Keynes and Rojas 1974). Adrian's subsequent calculations make use of the Hodgkin and Huxley equations modified to include explicitly the effect of gating current (Adrian 1975). Adrian's calculations, although agreeing with Hodgkin's range of optimum channel densities, do not compute conduction velocity for propagating action potentials in the same manner as Hodgkin and Huxley (1952). Instead, the velocities are obtained approximately by measuring the initial exponential rates of depolarization at the foot of the action potential from a model of a space-clamped axon. Somewhat distressingly, this approach yields a maximum velocity according to Adrian of 14.7 m/s (at 18.5°C). The value is a full 30% below the experimental conduction velocity of 21.2 m/s.

In this paper, we reexamine the question of Hodgkin's maximum velocity hypothesis using an alternative approach that models gating current using an explicit time-varying gating capacitance. In addition, because this optimization question is parametrically sensitive, we seek a Hodgkin–Huxley-type

Address for reprint requests and other correspondence: William B Levy, University of Virginia Health System, Department of Neurosurgery, P.O. Box 800420, Charlottesville, VA 22908-0420 (E-mail: wbl@virginia.edu).

The costs of publication of this article were defrayed in part by the payment of page charges. The article must therefore be hereby marked "advertisement" in accordance with 18 U.S.C. Section 1734 solely to indicate this fact.

model that accurately reflects the critical variable—that is, the model must get conduction velocity right. Thus, we make several modifications—most suggested by Hodgkin and Huxley—that bring the computed action potential into better agreement with the experimental measurements.

### The standard HH model

The success and universal appeal of the Hodgkin–Huxley (HH) model is evident, 50 years later, by its repeated use as the prototypical model of excitation among many classes of electrically excitable cells. Hodgkin–Huxley-type models have been used to quantitatively describe the myelinated nerve axon of the frog sciatic nerve (Frankenhaeuser and Huxley 1964), striated muscle fibers (Adrian et al. 1970), and cardiac Purkinje fibers (McAllister et al. 1975). As a semiempirical deduction based on voltage-clamp experiments performed on the giant axon of *Loligo*, the Hodgkin–Huxley model (1952) has been able to account for most of the major features of nerve conduction, with the exception of accommodation (Jakobsson and Guttman 1980). The most startling aspect of the model has, no doubt, been its ability to make a reasonably accurate prediction of the conduction velocity of a propagating action potential using voltage–current measurements of a space-clamped axon as a starting point.

In the years since Hodgkin and Huxley introduced their model, the use of new and powerful experimental techniques has allowed an emergent microscopic picture of channel structure and function that conflicts with the corresponding microscopic properties that are implied by a literal interpretation of the HH model. In particular, precise measurements of  $\text{Na}^+$  gating current have shown that the inward gating current decays with the same time course as  $\text{Na}^+$  ion current (Armstrong and Gilly 1979), and not at 1/3 the rate as would have to be the case for Hodgkin–Huxley's 3-independent-particles picture of  $m^3$  activation. Furthermore, the HH model predicts a gating current associated with inactivation, although no gating current with the same time course as inactivation was ever found (Armstrong and Bezanilla 1977). In fact, inactivation reduces the inward gating current that is associated with channel closing (Armstrong and Bezanilla 1977) and refutes the basic claim that inactivation and activation occur independently (Armstrong 1992). In the case of  $\text{K}^+$  channels, the delayed onset of  $\text{K}^+$  current that is prolonged even more by a very hyperpolarized holding potential (the Cole–Moore shift) cannot be explained by the Hodgkin–Huxley model (Cole and Moore 1960). In addition, detailed measurements of gating current have allowed a significant advancement in the kinetic descriptions of channel activation for both  $\text{Na}^+$  channels (Armstrong and Gilly 1979; Keynes 1992; Patlak 1991; Vandenberg and Bezanilla 1991) and  $\text{K}^+$  channels (Clay 1995; Zagotta et al. 1994) and the gating current themselves.

In addition to these microscopic inaccuracies there are macroscopic inaccuracies, as mentioned by Hodgkin and Huxley themselves (Hodgkin and Huxley 1952). For the recorded action potential, there are clear discrepancies. Figure 1 compares the Hodgkin–Huxley model at 18.5°C (reproduced exactly using NEURON) with the experimental trace at 18.5°C scanned from Fig. 15c from Hodgkin and Huxley (1952). The

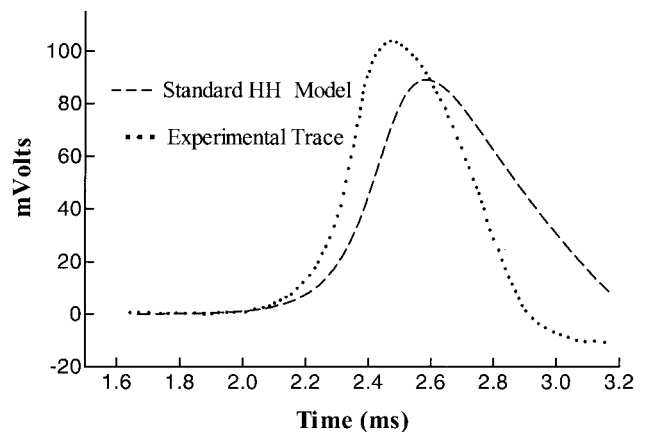


FIG. 1. Experimental trace of the action potential and the Standard HH model (digitally scanned from Hodgkin and Huxley, 1952, Fig. 15c). AP rises more rapidly, has greater overshoot, and has a greater propagation velocity than the standard HH model at 18.5°C (reproduced using NEURON). The computed velocity is 18.7 m/s and the experimentally recorded velocity is 21.2 m/s.

Hodgkin–Huxley model action potential depolarizes less rapidly, it has a smaller amplitude, and has a reduced propagation velocity (smaller by 11%). In addition, the repolarization phase of the recorded action potential trace is much more rapid than the model. The reasons for these discrepancies were not unknown to Hodgkin and Huxley. As they point out: 1) the model predicts too much  $\text{K}^+$  exchange and too little  $\text{Na}^+$  exchange; 2) the model has a peak that is too short, too sharp, and rises too slowly; and 3) the model does not sufficiently account for the initial delay ( $\sim 0.5$  ms for large depolarization at 6°C) in the  $\text{K}^+$  activation curve (Hodgkin and Huxley 1952, Fig. 3). According to Hodgkin and Huxley, poor representation of the initial  $\text{K}^+$  delay undoubtedly contributes to the poor shape of the action potential (mentioned in point 2). We take their suggestions as a starting point for improving the model.

Despite the shortcomings of the Hodgkin–Huxley model, its validity remains solid in the sphere of application that does not concern itself with the precise details of channel function. That is, with some modification, the macroscopic properties of the Hodgkin–Huxley model can effectively be used to test Hodgkin's evolutionary hypothesis that the squid is optimized for maximum conduction velocity alone. In particular, by adjusting the model to remove the inaccuracies of the velocity-dependent rising phase, we can accurately evaluate Hodgkin's optimization hypothesis.

We improved the model by adjusting the delayed onset of  $\text{K}^+$  conductance and by adjusting the voltage dependence of the  $h$ -inactivation rates (reverse reaction). As a result, the computed action potential now closely reproduces the rising phase of the biological action potential. In addition, the propagation velocity (at 18.5°C) has been raised from 18.7 m/s (standard HH) to 21.9 m/s (modified model), a value that compares nicely to the experimentally measured value of 21.2 m/s. With the reparameterized model, we can determine the optimal range of channel densities that maximizes velocity with some assurance of satisfactory accuracy, and Hodgkin's hypothesis is rejected. Because the optimum channel density predicted by Hodgkin's maximal velocity hypothesis is more

than twice as high as the experimental estimate (or 4 times too high when the reduced gating capacitance approximation to the serial model is incorporated), we present alternative candidates for an optimization criterion that includes, in particular, energy efficiency (Attwell and Laughlin 2001; Laughlin and Sejnowski 2003; Levy and Baxter 1996).

## METHODS

We have simulated propagating action potentials and calculated their properties using the simulation environment NEURON (Hines and Carnevale 1997). Preliminary experiments in some of the modeling studies were performed with NeuroDynamix (Friesen and Friesen 1994). Apart from channel-specific properties that were changed from the standard Hodgkin–Huxley model, all aspects of our simulated axon were chosen to reproduce the geometry and passive electrical characteristics of the squid giant axon. In addition to describing channel-specific alterations, the details of exploring the dependence of propagation velocity on both  $K^+$  conductance delay and the  $Na^+$  channel density will be summarized.

The simulated axon used in all cases was as similar as possible to the squid giant axon used in Hodgkin–Huxley simulations (1952). The axon diameter and length were 476  $\mu\text{m}$  and 10 cm, respectively. The Nernst potentials for  $Na^+$  and  $K^+$  were +50 and  $-77$  mV, respectively. The resting potential was always fixed at  $-65$  mV. When necessary (i.e., whenever channel properties were changed), the leak potential was adjusted so that  $g_K(V_m - E_K) + g_{Na}(V_m - E_{Na}) + g_L(V_m - E_L) = 0$ . For the final reparameterized model, the leak potential was maintained at  $-69$  mV throughout the course of each simulation.

The number of conjoined segments making up the axon varied from 500 to 3,000 and the time step used for integrating the cable equation varied from 1 to 25  $\mu\text{s}$ , depending on the resolution needed for the particular simulation. The highest-resolution simulations showed that the accuracy of the results using the Crank–Nicholson integration scheme was insensitive to the longest time step used (25  $\mu\text{s}$ ).

All measurements made during the course of a simulation were made in the steady state when the action potential had propagated at least 5 cm down the axon (several space constants). As the propagating wavefront traveled down the axon, the time and position of an arbitrary depolarization level ( $-50$  mV) were recorded. Because of the invariance of the shape of a traveling wave, it did not matter whether we recorded the speed at the peak or at the foot of the action potential. Specifically, the time interval between the 6-cm position and the 8-cm position was recorded and the velocity was then calculated. The steady-state condition (traveling wave assumption) was separately verified by repeating the calculation for very long axons (up to a meter) with no change in conduction velocity.

As active components anchored within the membrane, the complex behavior of voltage-gated ion channels determines most of the interesting and biologically important properties of the action potential. According to Hodgkin and Huxley, the opening of  $K^+$  channels is controlled by the presence of 4 charged activating  $n$  particles (or dipoles), whose traversal across the membrane induces the necessary conformational changes within the channel protein to allow  $K^+$  ions to flow to the outside of the membrane. In the case of  $Na^+$  channels, the independent movements of 3 activating  $m$  particles, in the absence of a fourth inactivating  $h$  particle, cause the opening of the channel. Each particle's independent probability of occupying an activated state is assumed to be dominated by first-order kinetics in a voltage-driven reaction with voltage-dependent rate constants. The combined probability for a channel being open in the case of  $K^+$  is  $n^4$  (standard HH), and in the case of  $Na^+$  it is  $m^3h$ , giving a  $K^+$  conductance of  $g_K = \bar{g}_K n^4$  and a  $Na^+$  conductance of  $g_{Na} = \bar{g}_{Na} m^3 h$ . In each case, the first-order rate equation for activation or inactivation is

$$dn/dt = (n_\infty - n)(\alpha_n + \beta_n)Q_{10} \quad (1a)$$

$$dm/dt = (m_\infty - m)(\alpha_m + \beta_m)Q_{10} \quad (1b)$$

$$dh/dt = (h_\infty - h)(\alpha_h + \beta_h)Q_{10} \quad (1c)$$

The temperature dependence of the rates is expressed in the term  $Q_{10} = 3^{(T-6)/10}$ . The voltage dependencies of the forward and backward rate constants ( $\alpha$  and  $\beta$ ) are

$$\alpha_n(V_m) = \frac{a_{n1}[-(V_m + 65) + a_{n2}]}{\exp\{[-(V_m + 65) + a_{n2}]/10\} - 1} \quad (2a)$$

$$\beta_n(V_m) = b_{n1} \exp[-(V_m + 65)/b_{n2}] \quad (2b)$$

$$\alpha_m(V_m) = \frac{a_{m1}[-(V_m + 65) + a_{m2}]}{\exp\{[-(V_m + 65) + a_{m2}]/10\} - 1} \quad (2c)$$

$$\beta_m(V_m) = b_{m1} \exp[-(V_m + 65)/18] \quad (2d)$$

$$\alpha_h(V_m) = a_{h1} \exp[-(V_m + 65)/20] \quad (2e)$$

$$\beta_h(V_m) = \frac{b_{h1}}{\exp[-(V_m + 65) + b_{h2}]/10 + 1} \quad (2f)$$

whose parameters have been left free for the purpose of subsequent discussion.

## The gating capacitance mechanism

Analogous to the base current of a transistor, the charge displacement of  $m$ ,  $n$ , and  $h$  particles gives rise to a gating current that is not included in the original Hodgkin–Huxley model. In proportion to the ionic currents that flow through the open channels, the gating current is negligible at all times except during the early rising phase of the action potential when the gating current accounts for a noticeable fraction of the total current through the membrane. The approach we use to model gating current makes use of voltage-dependent capacitance measurements and requires no specific knowledge of the number and charge of the activating particles. We assume, however, that the gating current during the early rising phase occurs with the same time scale as  $m$  particle displacement (Eq. 1b).

In the most general, model-independent language, the activation of voltage-gated ion channels occurs through voltage-induced conformational changes of charged segments within the channel protein. The net charge displacement of the protein segments during a time  $\Delta t$  may be thought of as either a gating current, or equivalently, as the effect of a continuously varying voltage-dependent capacitance. Specifically, we can write  $Q_g$  (gating charge/cm<sup>2</sup>) and the correspondence between gating capacitance and gating current as

$$Q_g(t) = C_g(t)V_m(t) \quad (3a)$$

$$I_g(t) = dQ_g(t)/dt = V_m(t)dC_g(t)/dt + C_g(t)dV_m(t)/dt \quad (3b)$$

Here,  $V_m$  is the membrane potential, with a resting potential of  $-65$  mV. In Eq. 3b, the 2 terms on the right, which result from the application of the product rule for derivatives to the expression  $Q_g(t) = C_g(t)V_m(t)$ , can be understood by imagining a special kind of capacitor that is able to change its properties during charging. Physically, the dielectric strength of the membrane reduces continuously during depolarization as the gating charge moves across the membrane. Thus we have the pure membrane capacitance and then a parallel capacitive current attributed to movement of the gating charge. In this case, the resulting current depends both on the instantaneous capacitance through  $C_g(t)dV_m(t)/dt$  and on the rate of change of capacitance through  $V_m(t)dC_g(t)/dt$ .

The total membrane capacitance is the sum of the variable gating capacitance  $C_g(t)$  and the voltage-independent membrane capacitance  $C_0$ . Measurements of the voltage-independent capacitance of 3 separate classes of neurons show the fixed membrane capacitance to be

close to  $0.9 \mu\text{F}/\text{cm}^2$  (Gentet et al. 2000). Fernandez et al. (1982) estimated for the squid giant axon that the maximum change of the voltage-dependent part of the capacitance  $C_{\text{Na}}^{\text{max}}$  at low frequency is about  $0.15 \mu\text{F}/\text{cm}^2$  in the steady state. We used a value of  $0.88 \mu\text{F}/\text{cm}^2$  for  $C_0$  [according to Gentet and consistent with Adrian's (1975) estimation for fixed membrane capacitance], and  $0.13 \mu\text{F}/\text{cm}^2$  for  $C_{\text{Na}}^{\text{max}}$ , to give a total membrane capacitance of  $1.01 \mu\text{F}/\text{cm}^2$  at the resting potential.

In our analysis, we have only considered the gating charges that accompany the opening of  $\text{Na}^+$  channels. In particular, we consider only the charge displacement of the  $m$  particles. We do not consider the displacement of the  $h$  particle because no gating current with the same time course as inactivation seems to exist (Armstrong and Bezanilla 1977). In addition, we have neglected the inclusion of  $\text{K}^+$  gating current in our gating current mechanism. Because the magnitude of  $\text{K}^+$  gating current is quite small [the number of  $\text{K}^+$  channels is only a fraction (1/12) of the number of  $\text{Na}^+$  channels] and has a time course that begins well after the early rising phase of the action potential,  $\text{K}^+$  gating currents have a negligible effect on the velocity-dependent features of the action potential.

Variable gating capacitance may be understood as being controlled by an abstract reaction coordinate that maps the extent that the gates have "swung" open. Upon depolarization, a fraction  $m$  of  $\text{Na}^+$  gating particles has traversed the membrane (in whole or in part), initiating a reduction of the total capacitance by an amount  $C_{\text{Na}}^{\text{max}} [1 - m(t)]$ . At a high enough holding potential, a fully open gate ( $m$  close to 1) has no capacitance.

In terms of the variable  $m(t)$  and the maximum change of the variable capacitance,  $C_{\text{Na}}^{\text{max}}$ , the gating current (Eq. 3b) becomes

$$I_g(t) = -V_m(t)C_{\text{Na}}^{\text{max}}dm(t)/dt + C_{\text{Na}}^{\text{max}}[1 - m(t)]dV_m(t)/dt \quad (4)$$

Adding the gating current in the Hodgkin–Huxley equation that describes the evolution of the action potential we have

$$\frac{a}{2R\theta^2} \frac{d^2V_m(t)}{dt^2} = C_{\text{Na}}^{\text{max}}[1 - m(t)] \frac{dV_m(t)}{dt} - C_{\text{Na}}^{\text{max}}V_m(t) \frac{dm(t)}{dt} + C_0 \frac{dV_m(t)}{dt} + \{\bar{g}_{\text{K}}n^4[V_m(t) - E_{\text{K}}] + \bar{g}_{\text{Na}}m^3h[V_m(t) - E_{\text{Na}}] + \bar{g}_{\text{L}}[V_m(t) - E_{\text{L}}]\} \quad (5)$$

where the variable  $R$  is the specific resistance of the axoplasm,  $a$  is the axon diameter, and  $\theta$  is the propagation speed. The original Hodgkin–Huxley equation can be recovered by setting the first 2 terms (r.h.s.) to zero, and changing  $C_0$  to  $1.01 \mu\text{F}/\text{cm}^2$ .

The effect of the gating capacitance mechanism is that it limits conduction velocity at large channel densities and is solely responsible for the existence of an optimum channel density—without it, the conduction velocity would be a monotonically increasing function of channel density.

### Incorporating modern $\text{Na}^+$ -channel observations

There are many characteristics of  $\text{Na}^+$  channel activation and inactivation that the Hodgkin–Huxley hypothesis missed (Patlak 1991; Vandenberg 1991). Most differences concern the time course of both ion currents and gating currents under voltage clamp, as well as the fact that gating currents do not simply constitute a monoexponential function of time. With one exception—the time course of gating capacitance—these differences will not significantly affect either the rising phase or the propagation velocity and can be modeled with a parallel model and still produce a satisfactory approximation. Modification of the gating-capacitance mechanism, as it turns out, can still be accommodated within the parallel model.

The gating-capacitance mechanism, based on a serial model of  $\text{Na}^+$  activation (Patlak 1991; Vandenberg and Bezanilla 1991), leads to a smaller available gating capacitance and a delayed time course of gating charge movement. In Patlak's model (*model number 8*, Patlak

1991), the initial gating current is reduced compared to the Hodgkin–Huxley value upon a voltage clamp pulse from  $-70$  to  $0$  mV and does not exceed the Hodgkin–Huxley prediction throughout the course of the voltage clamp. We incorporated this reduced available gating capacitance of Patlak's serial model by reducing the available gating capacitance to  $0.08 \mu\text{F}/\text{cm}^2$ , which is two-thirds of the low-frequency value given by Fernandez et al. We also explored the latency of the gating capacitance by adjusting the time at which the gating capacitance decreases.

### Artificial delay of $\text{K}^+$ conductance

Hodgkin and Huxley pointed out that the family of experimental  $\text{K}^+$  conductance curves (Fig. 3 from Hodgkin and Huxley 1952) displays an initial delay that is not adequately represented by the model's  $\text{K}^+$  conductance curves. This effect is particularly noticeable for large clamping voltages (up to  $0.5$  ms at  $6^\circ\text{C}$  at large depolarization) and as a result, the absence of this experimentally observed delay may significantly influence the shape and height of the action potential in the vicinity of maximum overshoot. In specific terms, the lack of initial delay of  $g_{\text{K}}$  tends to increase the overlap of  $\text{K}^+$  and  $\text{Na}^+$  currents throughout the course of the action potential to a greater extent in the model than in a giant axon.

To evaluate a role of the overlap during the rising phase, we use the artifice of a forced  $g_{\text{K}}$  delay as a tunable parameter. In particular, we explore the effect of  $g_{\text{K}}$  delay on the propagation velocity of the action potential. We note that we did not use forced  $g_{\text{K}}$  delay as a component of the final modified model, but rather to emphasize the consequences of reducing the overlap of  $\text{K}^+$  and  $\text{Na}^+$  currents (e.g., increased rate of rise, peak height, and velocity). We then show that increasing the  $g_{\text{K}}$  activation exponent from 4 to 6 reproduces these benefits.

According to the Hodgkin–Huxley model,  $g_{\text{K}}$  conductance is proportional to  $n^4$ , and at a fixed clamping potential,  $n$  rises exponentially according to Eq. 1a. It is true that as the exponent of  $g_{\text{K}}$  conductance is increased, the S-shape of the  $g_{\text{K}}$  activation curve shows more of an initial delay. Indeed, Cole and Moore succeeded in matching the  $\text{K}^+$  activation curves very well using a system with as many as 25 particles:  $g_{\text{K}} = \bar{g}_{\text{K}}n^{25}$  (Cole and Moore 1960). However, such a large number of activating particles that move fully across the membrane does not seem probable and is not supported by gating current measurements (Hoyt 1963).

By manipulating Eq. 1a during the course of the action potential, the  $\text{K}^+$  conductance can be maintained at its resting value for a fixed length of time, enforcing an arbitrary delay. In practice, we implement the effect of a delay by setting Eq. 1a to zero until a fixed arbitrary time has passed, at which point the  $\text{K}^+$  activation is "switched on" and allowed to develop in time according to Eq. 1a

$$\begin{aligned} dn/dt &= 0 & \Delta t < t_{\text{delay}} \\ dn/dt &= (n_{\infty} - n)(\alpha_n + \beta_n)Q_{10} & \Delta t > t_{\text{delay}} \end{aligned} \quad (6)$$

Because time is a global variable that does not change from one position to another along the axon, we cannot use absolute time to determine when the restriction to Eq. 1a should be lifted. Instead, we use a predetermined level of depolarization as a *trigger* that signals the time  $t_f$  at which  $\text{K}^+$  conductance should locally be turned on. Delay time  $\Delta t$  is measured by recording the times  $t_0$  at which the membrane has depolarized to  $0.1$  mV above resting potential and  $t_f$ , the time at which the membrane has depolarized to the "trigger" level. It is true that using the  $0.1$  mV level to define  $t_0$  is somewhat arbitrary. However, for our present purposes, we need to compare only the relative effect of increased delay on propagation velocity, and a rigorous measure of delay is not necessary.

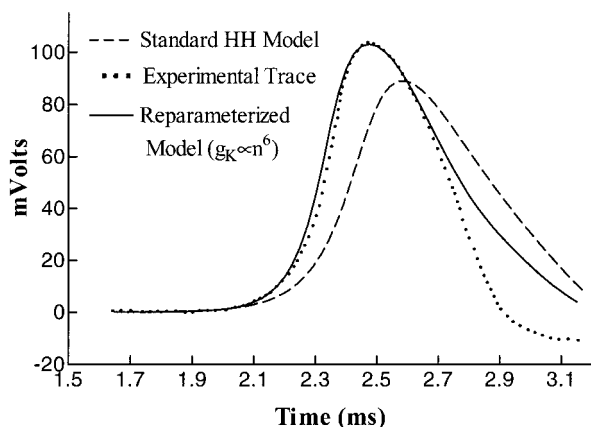


FIG. 2. Improved parameterization (see Table 1, improved model I). Comparison of the improved parameterization (best-fit model) to experimental action potential and to the Hodgkin-Huxley 1952 parameterization is shown (18.5°C). The improved model uses 1) variable gating capacitance, 2) a 6-particle  $K^+$  activation system, and 3) altered  $h$ -inactivation kinetics to produce a waveform that closely agrees with the rising phase of the recorded action potential. The improved model fits the rising phase nearly perfectly and possesses better agreement with the falling phase, whereas the original model rises and falls too slowly, and has a reduced peak height. The computed velocity of the improved model is 21.9 m/s (compare to 21.2 m/s for the experimental trace). There is no fixed delay included in this parameterization.

## RESULTS

### The improved model

In Fig. 2, our final improved model (see Table 1, *Improved Model I*) is compared to the *experimental trace*. The agreement is nearly exact during the rising phase and is even slightly improved during the repolarization phase. The propagation speed of 21.9 m/s more closely approximates the measured experimental value of 21.2 m/s at 18.5°C. The improved model consists of 3 main alterations whose individual contributions are detailed below. Although the introduction of the gating current mechanism had little effect on the shape and speed of the action potential at the standard channel density, its effect is pronounced at small and large channel densities. The other 2 main alterations—reparameterized  $h$ -inactivation rates and a 6-particle  $K^+$  activation system—both contributed significantly to the improvement of the shape and speed of the action potential. Even though we have not been explicitly interested in fitting the falling phase, it is clear that the reparameterized model is improved, relative to the recorded action potential, even significantly beyond the peak of the action potential. This

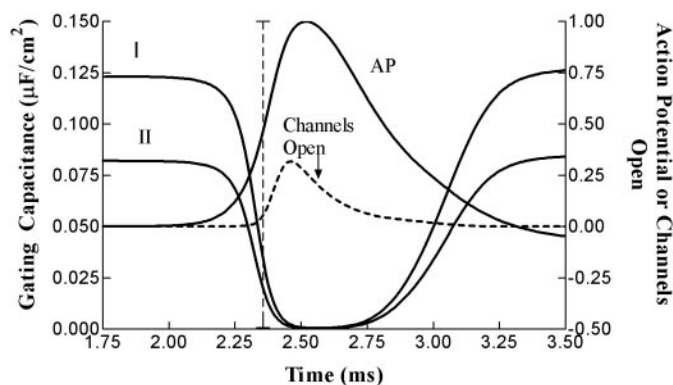


FIG. 3. Gating capacitance during AP. The time-course of the gating capacitance is shown for both the gating mechanism (used in all simulations, *curve I*) and the serial approximation (*curve II*). *Dashed curve* shows the fraction of channels that are open during the course of the action potential. Note that very few channels have opened before the maximum rate of rise of the action potential, well before the turnoff of the gating capacitance. Action potential is plotted as a fraction of the peak maximum.

feature seems to be a consequence of the 6-particle activation system either as an increased  $g_K$  delay, or a more rapid turning on of the  $K^+$  channels. The importance of the  $g_K$  delay will be explored further by introducing an artificial delay as an adjustable parameter. Table 1 summarizes the altered parameterizations.

### Gating current mechanism

The impact of the gating current mechanism on the standard Hodgkin-Huxley model was slight at normal channel densities. Its inclusion, however, is merited by the well-established observation of gating currents and variable gating capacitance in the squid giant axon. Furthermore, a model that also accounts for gating current is absolutely necessary for a critical analysis of Hodgkin's maximum velocity hypothesis.

The most relevant aspects of the gating current mechanism are shown in Fig. 3. As described in METHODS the total membrane capacitance is composed of the fixed membrane capacitance ( $0.88 \mu\text{F}/\text{cm}^2$ ) and the variable gating capacitance that varies continuously from  $0.13$  to nearly  $0 \mu\text{F}/\text{cm}^2$  during the course of the action potential. Similarly, in the modern serial  $\text{Na}^+$  channel model, capacitance varies continuously but the starting value and time course are defined by Patlak's model (*model number 8*, Patlak 1991). Shown in the figure is the

TABLE 1. Summary of model parameters

Model	$\bar{g}_{\text{Na}}, \text{S}/\text{cm}^2$	$b_{h1}, 1/\text{ms}$	$b_{h2}, \text{mV}$	$n$ -Exponent	Gating Mechanism
Hodgkin-Huxley (Fig. 1)	0.12	1	30	4	no
Improved Model I (Fig. 2)	0.13	1.8	49	6	yes
Gating capacitance (Fig. 3)	0.12	1	30	4	yes
Serial approx. (Fig. 3)	0.12	1.65	49	5.8	yes
					(Reduced to 2/3)
$K^+$ activation (Fig. 4)	0.12	1	30	4, 5, 6	yes
Artificial delay (Fig. 5)	0.12	1	30	4, 5, 6	yes
$h$ -Inactivation (Fig. 6)	0.12	1.8	49	4	yes
Improved Model II (Fig. 7, 8)	0.12	1.6	49	5.8	yes
Velocity (18.5°C) (Fig. 9)	(0.04–0.5)	1.8	49	6	yes
Velocity (5°C) (Fig. 10)	(0.04–0.5)	1.6	49	5.8	yes

gating-capacitance mechanism that we have used in almost all of our simulations (*curve I*) as well as the serial approximation that uses two-thirds of the low-frequency limit (*curve II*) of the gating capacitance. The vertical dashed line reveals that very few channels (<10%) have opened before the action potential has reached maximum rate of rise. This is an important observation because it indicates that there is considerable room for a temporal shift of the time when the gating current goes to zero (as we would expect in a serial model) that will have no effect on the velocity. What only seems to matter is the early reduction in capacitance, and separate unpublished simulations altering the delay in the time of capacitance reduction have confirmed this insight. By delaying the time at which the gating capacitance begins to approach zero, we saw that the conduction velocity of the action potential was only slightly affected. (We note that a separate reparameterization of the *h*-inactivation rates was required to bring the serial approximation into agreement with the physiological measurements of the squid action potential; see Table 1).

The gating current initially counteracts the  $\text{Na}^+$  current at the foot of the action potential, causing the initial depolarization to be retarded relative to the standard Hodgkin–Huxley model, which does not include a gating mechanism. Shortly beyond the foot, the gating capacitance dips nearly to zero and the effect of a reduced gating capacitance,  $C_{\text{Na}}^{\text{max}} [1 - m(t)]$ , allows the axon membrane to depolarize more rapidly, giving it a slightly higher peak. The propagation speed of an action potential is roughly proportional to  $1/\sqrt{C_m}$ ; however, at the actual channel density, the reduced overall capacitance of the membrane at large depolarization does not increase the action potential's speed as one might suppose. In fact, the initial surge of gating current neutralizes the effect of a reduced capacitance, slightly lowering the action potential's velocity to 18.6 m/s. The difference between the shape of the standard Hodgkin–Huxley action potential with and without the gating mechanism included is so slight that a comparison has not been shown. However, it must be emphasized that this is true only for the biological channel densities used in the 1952 Hodgkin–Huxley model ( $\bar{g}_{\text{K}} = 0.036 \text{ S/cm}^2$  and  $\bar{g}_{\text{Na}} = 0.12 \text{ S/cm}^2$ ). The effect of the gating capacitance mechanism can be appreciated by noting that without it conduction velocity would be a monotonically increasing function of the channel density (Hodgkin 1975) and would not exhibit a rounded peak as shown in Figs. 9 and 10.

In addition to having introduced gating capacitance into the model, we outline in the next 2 sections a reparameterization strategy that is consistent with 2 main ideas discussed by Hodgkin and Huxley: the extent of  $g_{\text{K}}/g_{\text{Na}}$  overlap is too great in the Hodgkin–Huxley standard model, and the exchange of  $\text{Na}^+$  near the  $\text{Na}^+$  reversal potential is too small. The chosen sets of parameters are not the only ones that produce a satisfactory fit of the rising phase of the experimental trace, although they are the most reasonable choices consistent with our strategy.

#### Delaying $g_{\text{K}}$

Hodgkin and Huxley (1952) noted that one of the shortcomings of their model is that the experimental  $g_{\text{K}}$  activation curve presents a noticeable initial delay for high clamping voltages that is not accurately represented by a 4-particle activation system ( $g_{\text{K}} = \bar{g}_{\text{K}}n^4$ ). They suggest that a 6-particle

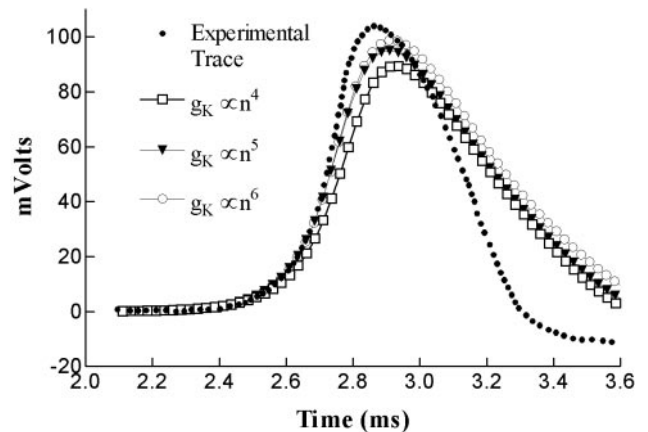


FIG. 4. Standard HH model with altered exponents of  $g_{\text{K}}$  activation ( $18.5^\circ\text{C}$ ). Increasing the exponent of  $g_{\text{K}}$  activation monotonically increases the action potential's height, rate of depolarization, and propagation speed. Even with an exponent of 6, however, the simulated action potential is still too small and rises too slowly. The propagation speed increases from 18.6 m/s at  $n = 4$  to 19.6 m/s at  $n = 6$ .

system with  $g_{\text{K}} = \bar{g}_{\text{K}}n^6$  could reproduce the desired effect. To understand Hodgkin and Huxley's thinking, note that the temporal overlap of  $g_{\text{K}}$  and  $\bar{g}_{\text{Na}}$  within the standard model (Hodgkin and Huxley 1952, Fig. 17) is quite significant. A feature of the Hodgkin–Huxley model is that this overlap (i.e., lack of delay) causes significant overlap of opposing  $\text{Na}^+$  and  $\text{K}^+$  currents. The overlap of opposing currents reduces the rate of initial depolarization and reduces the propagation velocity of the modeled action potential, and is also energetically wasteful.

Figure 4 demonstrates the effect that the exponent of  $n$  has on the modeled action potential. Shown are 3 curves, in addition to the *experimental trace*. The only difference between these simulated action potentials is the exponent of  $g_{\text{K}}$  activation. (All other parameters used to generate these curves are exactly the same as in the standard Hodgkin–Huxley model with the addition of the previously described gating current mechanism.) As the power of  $n$  is increased successively from 4 to 6, the delay between  $g_{\text{K}}$  and  $g_{\text{Na}}$  increases, and the action potential progressively becomes steeper, larger, and faster. The speed of the action potential increases monotonically with  $n$  from 18.6 m/s at  $n = 4$  to 19.5 m/s at  $n = 6$ .

To examine directly the effect of delay on propagation velocity, we systematically restrain  $g_{\text{K}}$  activation for a fixed delay period as described in METHODS. We see in Fig. 5 that propagation velocity is a monotonic function of  $g_{\text{K}}$  delay for each exponent of activation. The propagation velocity is very sensitive to  $g_{\text{K}}$  delay, as may be observed by noting that it rises over a narrow region of approximately 200  $\mu\text{s}$ . This is consistent with the observed initial  $g_{\text{K}}$  delay that can be described from the family of voltage-clamp curves in Fig. 3 of Hodgkin and Huxley (1952), if we assume  $Q_{10} = 3$  and adjust for temperature. Most important, we see that the impact of  $g_{\text{K}}$  delay is most significant in the case of the 4-particle activation system, and becomes less significant as the  $g_{\text{K}}$  activation exponent is increased. We can conclude that the 6-particle system already manifests a significant  $g_{\text{K}}$  delay that cannot be greatly improved upon even by forcibly extending the delay. Having demonstrated that the essential benefit of  $n^6$  activation kinetics is that it provides the necessary  $g_{\text{K}}$  delay, it was not necessary to incorporate fixed delay into the reparameterized model.

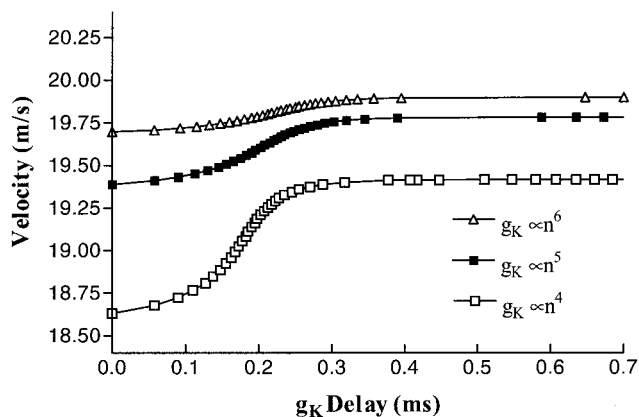


FIG. 5. Velocity dependence of forced  $g_K$  delay for several exponents of activation. The effect of increasing forced  $g_K$  delay is to increase the height and velocity of the action potential. The observed enhancement of velocity due to  $g_K$  delay is greatest for the 4-particle system and least for the 6-particle system that is used in Fig. 4 and the best-fit model of Fig. 2. Because of the delay produced by increasing the exponent of  $n$ , the 6-particle system already manifests an initial delay whose effect on velocity is largely saturated.

#### Modification of $h$ -inactivation parameters

The combined effect of a higher-order  $g_K$  activation system and gating capacitance substantially improves the model's comparison to the *experimental trace*, yet further avenues for refinement exist in the modification of the rate constants that govern the  $\text{Na}^+$  and  $\text{K}^+$  channel kinetics. In particular, because the empirical determination of  $\alpha_h(V_m)$  and  $\beta_h(V_m)$  is based on data with a severe degree of scatter (Fig. 9 in Hodgkin and Huxley 1952), the functional form of the rate constants for the  $h$ -system kinetics (Hodgkin and Huxley 1952; *Eqs. 23 and 24*) appears to admit some flexibility of choice.

In fact, one of the most significant improvements of the model came from solely altering the  $h$ -system kinetics. The voltage dependence of the  $h$ -inactivation rates was altered by choosing the parameters in *Eq. 2* as  $b_{h1} = 1.8$  and  $b_{h2} = 49$ , whereas  $a_{h1}$  and  $a_{h2}$  were left unchanged from the standard Hodgkin–Huxley model (i.e., we altered only the backward reaction rate of the  $h$ -inactivation particle). Increasing the numerator  $b_{h1}$  in *Eq. 2f* and shifting the voltage dependence ( $b_{h2}$ ) forward by 20 mV effectively retards  $h$ -inactivation for a longer time. In addition to allowing more  $\text{Na}^+$  to flow near the peak of the action potential, the effective delay in inactivation is consistent with the observations of recovery from inactivation using a double-pulse protocol (Armstrong and Bezanilla 1977; Goldman and Schauff 1972; Kuo and Bean 1994). One may observe from Fig. 6 that a partial improvement occurs when only the  $h$ -system kinetics are altered. Now, the rate of depolarization nearly matches the *experimental trace*, but the action potential does not have the proper overshoot amplitude.

An initial investigation revealed that alteration of the voltage dependence of the  $n$ -system activation rates [i.e.,  $\alpha_n(V_m)$  and  $\beta_n(V_m)$ ] did not significantly affect the shape and speed of the rising phase of the action potential. Consequently, the  $n$ -system rate parameters were left unchanged. Because propagation velocity is exclusively derived from parameters that control the rising phase, we have not considered  $\text{K}^+$  activation rates beyond the aspect of increasing  $g_K$  delay.

#### Combined improvements

The improved parameterization shown in Fig. 2, which combines each of the 3 improvements discussed above, is not the only parameterization that fits the rising phase of the experimental trace. An even better fit to the rising phase can be obtained by slightly reducing the  $n$  exponent of activation from 6 to 5.8. Conformational changes within the channel protein involve charge movements that may traverse all or part of the membrane potential. In this sense, a fractional number of activating “particles” represents the conformational change as the continuous motion of a charged dipole through the membrane. A second improved model that uses an exponent of 5.8 is shown in Fig. 7 at a temperature of 18.5°C.

To further evaluate the validity of all these changes, we tested the improved model (using  $g_K = \bar{g}_K n^{5.8}$ ) at a temperature of 5°C and compared (Fig. 8) the results to the *experimental trace* obtained from Hodgkin and Katz (1949). Again, there is an excellent agreement with the rising phase of the action potential (the agreement is nearly as good when using  $g_K = \bar{g}_K n^6$ ). The agreement of the model with the rising phase of each *experimental trace* over this particularly relevant temperature range lends credibility to the modifications, and it now seems appropriate to analyze Hodgkin's maximum velocity hypothesis.

#### Comparing channel density to Hodgkin's maximal velocity hypothesis

Using the improved model that combined a 1) 6-particle  $g_K$  activation system, 2) altered  $h$ -inactivation rates, and 3) a gating-capacitance mechanism,  $\text{Na}^+$  channel density was varied over a wide range, and conduction velocity was calculated at each value. Presumably, according to Hodgkin (1975), the channel density at which velocity is maximal should agree with the channel density of the squid.

To avoid the snare of comparing theoretical values of the squid channel density to the wide variation of reported values in the literature, we used the reported values of the  $\text{Na}^+$  gating

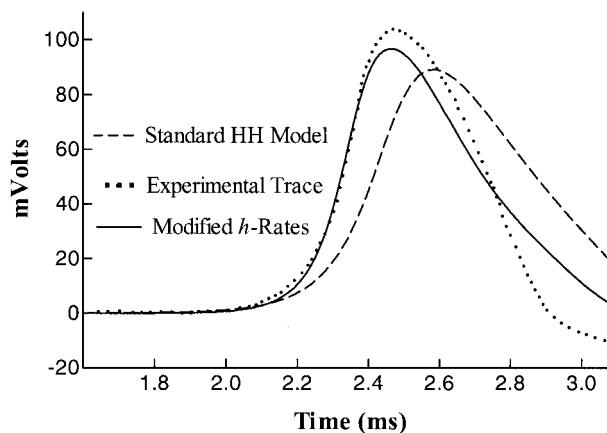


FIG. 6. Standard HH model with altered rates of  $h$ -inactivation (18.5°C). Alteration of  $h$ -inactivation kinetics alone significantly improves the shape and speed of the action potential. Altering the voltage-dependence of the backward rate expressions for  $\text{Na}^+$  inactivation has the effect of retarding inactivation and prolonging  $\text{Na}^+$  current near the peak of the action potential. The modified action potential agrees nearly exactly with the *experimental trace* during much of the rising phase but has an overshoot amplitude that is too small. This parameterization produces a propagation velocity of 20.8 m/s.

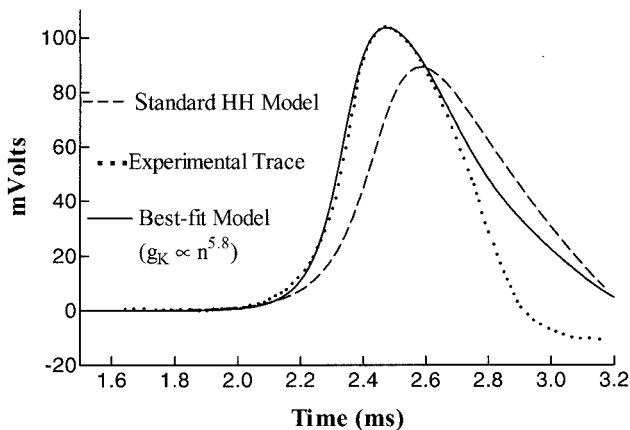


FIG. 7. Improved parameterization at 18.5°C (see Table 1, *improved model II*). A reparameterization based upon a slightly smaller  $n$ -exponent of 5.8 in addition to the other modifications (gating-capacitance mechanism, altered  $h$ -inactivation rates) reveals an even better fit of the rising phase at 18.5°C. The fractionation of the exponent of  $g_K$  activation is justified by the fact that charge relocations within the membrane do not necessarily fully traverse the membrane and do not see the full membrane potential.

capacitance and maximum  $\text{Na}^+$  conductance themselves. That is, we associate channel density as a relative quantity with the empirical measures of gating capacitance and maximal  $\text{Na}^+$  conductance per square micron. Specifically, the pure membrane capacitance is  $0.88 \mu\text{F}/\text{cm}^2$ , whereas the contribution of the variable gating capacitance is  $0.13 \mu\text{F}/\text{cm}^2$  (Gentet 2000; Fernandez 1982). The total capacitance at an arbitrary channel density is  $C_{\text{rest}} = C_0 + C_{\text{Na}}^{\text{max}} = 0.88 + 0.13\eta$ , where  $\eta$  is the relative channel density that is normalized by the channel density of the squid. Similarly the macroscopic conductance is given by  $g_{\text{Na}} = \bar{g}_{\text{Na}}\eta$ , where  $\bar{g}_{\text{Na}}$  is taken to be the widely established maximum  $\text{Na}^+$  conductance with a value of  $0.12 \text{ S}/\text{cm}^2$ .

The optimization for velocity of the improved model does not coincide with the experimentally observed total capacitance ( $1.01 \mu\text{F}/\text{cm}^2$ ), and thus we question the validity of Hodgkin's maximum velocity hypothesis. Figure 9 is a plot

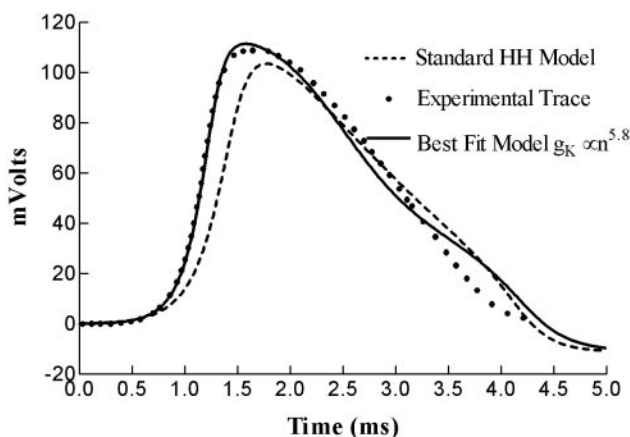


FIG. 8. Improved parameterization at 5°C (see Table 1, *improved model II*). The reparameterized model shown in Fig. 7 is computed at 5°C and compared to the *experimental trace* (Hodgkin and Katz 1949) and the standard HH model computed at 5°C. The modified model has near perfect agreement with the rising phase of the *experimental trace*, demonstrating that the reparameterization also works at the lower extreme of the biological temperature range. The reparameterization of Fig. 2 (see Table 1, *improved model I*) generated similar results.

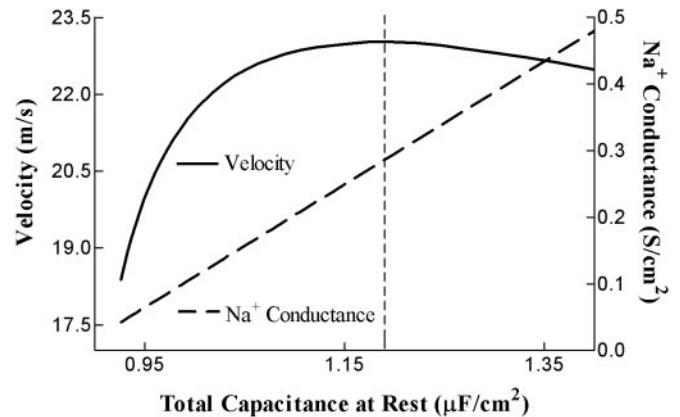


FIG. 9. Maximal velocity at optimal capacitance ( $\text{Na}^+$  conductance) for the *improved model II* at 18.5°C. The maximal velocity at optimum channel density according to Hodgkin's maximal velocity hypothesis predicts a resting capacitance that is too high ( $\sim 1.18 \mu\text{F}/\text{cm}^2$ , or a resting  $\text{Na}^+$  conductance of  $0.286 \text{ S}/\text{cm}^2$ ). To compare, the resting  $\text{Na}^+$  conductance and corresponding total capacitance for the squid (at resting potential) are  $0.12 \text{ S}/\text{cm}^2$  and  $1.01 \mu\text{F}/\text{cm}^2$ , respectively. Both  $\text{K}^+$  and leak channel density were increased in proportion with the  $\text{Na}^+$  channel density to maintain a resting potential of  $-65 \text{ mV}$ .

similar to the ones shown by Adrian and by Hodgkin (Adrian 1975; Hodgkin 1975). The important difference is that our calculations are based on propagating action potentials with a voltage-dependent gating-capacitance mechanism. When propagation velocity is plotted against the resting membrane capacitance (i.e., channel density is varied), we see that the maximum velocity occurs at  $1.18 \mu\text{F}/\text{cm}^2$ , and not the experimentally established  $1.01 \mu\text{F}/\text{cm}^2$ , giving a relative channel density of  $\eta = 2.5$ . Likewise, Hodgkin's optimization hypothesis applied at 5°C in Fig. 10 reflects nearly the same disagreement between estimated and experimentally observed channel densities. The predicted relative channel density for maximum velocity is  $\eta = 2.14$ , giving a total capacitance of  $1.15 \mu\text{F}/\text{cm}^2$ , again more than twice as high as the squid channel density.

Finally, we emphasize that these calculations underestimate

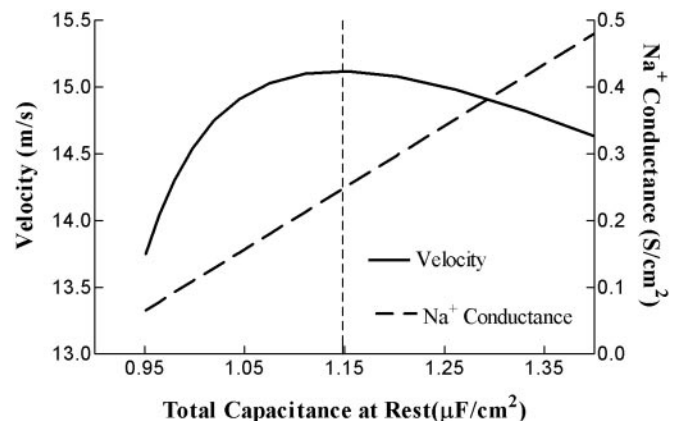


FIG. 10. Maximal velocity at optimal capacitance ( $\text{Na}^+$  conductance) for the *improved model II* at 5°C. Similar to Fig. 9, the optimum channel density that maximizes conduction velocity at 5°C predicts a resting capacitance of  $1.15 \mu\text{F}/\text{cm}^2$  or a resting  $\text{Na}^+$  conductance of  $0.249 \text{ S}/\text{cm}^2$ . Hodgkin's hypothesis applied at 5°C is not significantly different from the case of 18.5°C. The resting  $\text{Na}^+$  conductance and corresponding total capacitance for the squid (at resting potential) is  $0.12 \text{ S}/\text{cm}^2$ , and  $1.01 \mu\text{F}/\text{cm}^2$ , respectively. Both  $\text{K}^+$  and leak channel density were increased in proportion with the  $\text{Na}^+$  channel density to maintain a resting potential of  $-65 \text{ mV}$ .

the failure of Hodgkin's hypothesis. A gating-capacitance model that exploits the empirical aspects of a modern serial model (see METHODS) predicts an optimal relative channel density of  $\eta = 4$ . This result can be considered the more accurate estimate of the optimum channel density under Hodgkin's maximal velocity hypothesis. Thus the serial mechanism of gating capacitance only strengthens our rejection of Hodgkin's maximum velocity hypothesis.

## DISCUSSION

The inaccuracy of the standard Hodgkin–Huxley model in the rising phase of the action potential limits the model's utility for evaluating Hodgkin's velocity optimization hypothesis. The features that control velocity (e.g., rate of rise and amplitude of overshoot) are not in good agreement with the recorded action potential. Hodgkin and Huxley point out these problems and suggest that the inaccuracies may arise from a failure, as suggested by their voltage-clamp data, to delay  $g_K$  sufficiently in the model. That is, premature  $g_K$  activation diminishes the rate of rise and overshoot, and as a result, it limits the conduction velocity of the action potential.

To correct for this premature  $g_K$  activation, Hodgkin and Huxley suggest increasing the exponent of  $g_K$  activation from 4 to 6. We have found that an exponent of 6 increases velocity, but further increases of this exponent have little additional effect on velocity. That is, raising the activation exponent delays  $g_K$  activation and increases the rate of rise, the overshoot amplitude, and the propagation speed.

Although the larger  $g_K$  exponent noticeably improved the rising phase, an even better fit to the *experimental trace* seemed possible. Thus we also have altered the backward rate of  $g_{Na}$  inactivation [ $\beta_h(V_m)$ ], retarding  $g_{Na}$  inactivation to produce a larger action potential. We justify this change by the significant scatter of the experimental data (Fig. 9 from Hodgkin and Huxley 1952), which permits some flexibility in the empirical formulation of the inactivation rate, and also by the improved fit itself. Manipulating only the inactivation rate,  $\beta_h(V_m)$ , produces a simulated action potential that agrees very closely with the rising phase of the *experimental trace* and with a propagation speed of 20.8 m/s, it nearly matches the experimental conduction velocity, although it does not match the overshoot amplitude (see Fig. 6).

Combining these 2 improvements—the altered  $g_{Na}$  inactivation rates and an exponent of 6 for  $g_K$  activation—provides a very accurate fit to the rising phase (and part of the falling phase) of the recorded action potential, matching rate of rise, overshoot amplitude, and conduction velocity (within 3% at 18.5°C). As a further qualification of this improved model, we have found that the same parameterization matches the rising phase equally well at 5°C as at the 18.5°C setting, the temperature values used for most modeling studies. Thus the new parameterization is arguably robust over the 2 extremes of the squid's natural range of temperature.

For our purposes here, the final and perhaps most important addition to the standard Hodgkin–Huxley model was the introduction of a continuously varying voltage-dependent capacitance to model the variable gating capacitance observed in the squid (Fernandez et al. 1982). Although this alteration did not induce a great change in the shape and speed of the action potential at the channel density of the squid ( $\eta = 1$ ), this

channel-dependent capacitance forms the basis of Hodgkin's optimization hypothesis because without it there would be no velocity limitation at high channel densities.

Hodgkin's maximum velocity hypothesis does not provide an adequate evolutionary explanation for the channel density of the squid. The disagreement between the predicted value of the channel density and the actual value persists under the assumption that the squid is optimized for maximum propagation velocity. By correcting for the inadequacies of the original model, such as rate of rise, peak height, and propagation speed, we have effectively ruled out such inaccuracies as a source of error for the failure of Hodgkin's prediction. Thus, we continue to question the validity of Hodgkin's hypothesis. As our study demonstrates, even with significant improvements in accuracy, the modified model does not significantly alter the prediction of the optimal channel density from the prediction using the original model. At 18.5°C the relative channel density  $\eta$  that produces the maximum velocity is  $\eta = 2.5$ , equivalent to a total resting capacitance of 1.18  $\mu\text{F}/\text{cm}^2$ . At 5°C, the hypothesis is equally unsupported, predicting an optimizing relative channel density of  $\eta = 2.14$ . Moreover, these values significantly reduce the optimal channel density revealed by our investigation using the serial model for capacitance. From this work, the more probable value of the optimal relative channel density appears to be around  $\eta = 4$ .

Such a large temperature-independent difference between the predicted and actual channel densities makes it difficult to argue that natural selection has simply maximized conduction velocity. Another consideration that lies beyond the scope of our present analysis is the possibility that the squid relies on spike train coding for its escape response instead of single spikes. Such an analysis would require detailed knowledge of spike train coding in the squid as well as a highly accurate fit of the falling phase. As a first guess, however, Hodgkin's hypothesis is sensible; and quite possibly, the addition of further constraints will lead to a prediction of the observed  $\text{Na}^+$  channel density.

In moving away from Hodgkin's maximum velocity hypothesis, we suggest that metabolic constraints should be considered. After all, energy generation and the required metabolism are major constraints on the ability of organisms to compete, and as well, they are constraints on the niches in which they can compete. For example, besides the obvious limitations of food supply, oxygen saturation levels in seawater could limit metabolism. Such limitations place a premium on energy efficiency not just for the giant axon but for all axons.

The exact scaling function that relates metabolic cost to conduction velocity needs to be developed. Nevertheless, the work here will help such calculations by providing a more accurate assessment of metabolic cost. As a relative measure of metabolic cost, the integrated flux of  $\text{Na}^+$  in the rising phase, in some perhaps incomplete sense, expresses a proportional cost of velocity. Comparing the 1952 Hodgkin–Huxley simulation to the improved model indicates a moderate error in energy calculations will occur using the old model. Specifically, the new model, with its reduced overlap between  $g_K$  and  $g_{Na}$  in the rising phase gives a 10% reduction in  $\text{Na}^+$ -based metabolic cost within the rising phase. Furthermore, the serial model approximation reduces the cost of the wavefront production by an additional 2%, yet in either case, when the velocities are correctly matched, the energetic savings is in-

created an additional 3%. Thus, we estimate the total energy savings for the improved model to be around 13%. In sum, more accurate energy values calculated in the rising phase are now possible. However, choosing the correct quantity to optimize is perhaps the most challenging requirement for applying an evolutionary perspective that assumes microscopic optimization of evolutionarily stable cellular functions. Indeed, a best function that accurately approximates—as a scalar quantity—the full sum of an organism's needs may be impossible to find.

#### GRANTS

This work was supported by National Institutes of Health Grants MH-63855 and RR-15205 to W. B. Levy, the Meade Munster Foundation, and by the Department of Neurosurgery at the University of Virginia.

#### REFERENCES

- Adrian RH.** Conduction velocity and gating current in the squid giant axon. *Proc R Soc Lond B Biol Sci* 189: 189–186, 1975.
- Adrian RH, Chandler WK, and Hodgkin AL.** Voltage clamp experiments in striated muscle fibers. *J Physiol* 208: 607–644, 1970.
- Armstrong CM.** Voltage-dependent ion channels and their gating. *Physiol Rev* 72: S5–S13, 1992.
- Armstrong CM and Bezanilla F.** Inactivation of the sodium channel. II. Gating current experiments. *J Gen Physiol* 70: 567–590, 1977.
- Armstrong CM and Gilly WF.** Fast and slow steps of sodium activation. *J Gen Physiol* 74: 691–711, 1979.
- Attwell D and Laughlin SB.** An energy budget for signaling in the grey matter of the brain. *J Cereb Blood Flow Metab* 21: 1133–1145, 2001.
- Barlow HB.** The size of ommatidia in apposition eyes. *J Exp Biol* 29: 667–674, 1952.
- Clay JR.** A simple model of K<sup>+</sup> channel activation in nerve membrane. *J Theor Biol* 175: 257–262, 1995.
- Cole KS and Moore JW.** Potassium ion current in the squid giant axon: dynamic characteristic. *Biophys J* 1: 1–14, 1960.
- Fernandez JM, Bezanilla F, and Taylor RE.** Distribution and kinetics of membrane dielectric polarization. II. Frequency domain studies of gating currents. *J Gen Physiol* 79: 41–67, 1982.
- Frankenhaeuser B and Huxley AF.** The action potential in the myelinated nerve fiber of *Xenopus laevis* as computed on the basis of voltage clamp data. *J Physiol* 171: 302–315, 1964.
- Friesen WO and Friesen JA.** *NeuroDynamix. Computer Models for Neurophysiology.* New York: Oxford Univ. Press, 1994.
- Gentef LJ, Stuart GJ, and Clements JD.** Direct measurements of specific membrane capacitance in neurons. *Biophys J* 79: 314–320, 2000.
- Goldman L and Schaaf CL.** Inactivation of the sodium current in *Myxicola* giant axons. Evidence for coupling to the activation process. *J Gen Physiol* 59: 659–675, 1972.
- Hines ML and Carnevale NT.** The NEURON simulation environment. *Neural Comput* 9: 1179–1209, 1997.
- Hodgkin AL.** The optimum density of sodium channels in an unmyelinated nerve. *Philos Trans R Soc Lond B Biol Sci* 270: 297–300, 1975.
- Hodgkin AL and Huxley AF.** A quantitative description of membrane current and its application to conduction and excitation in nerve. *J Physiol* 117: 500–544, 1952.
- Hodgkin AL and Katz B.** The effect of temperature on the electrical activity of the giant axon of the squid. *J Physiol* 109: 240–249, 1949.
- Hoyt RC.** The squid giant axon, mathematical models. *Biophys J* 3: 399–431, 1963.
- Jakobsson E and Guttman R.** The standard Hodgkin–Huxley model and squid axons in reduced external Ca<sup>++</sup> fail to accommodate to slowly rising currents. *Biophys J* 31: 293–298, 1980.
- Keynes RD.** A new look at the mechanism of activation and inactivation of voltage-gated ion channels. *Proc R Soc Lond B Biol Sci* 249: 107–112, 1992.
- Keynes RD and Rojas E.** Kinetics and steady-state properties of the charged system controlling sodium conductance in the squid giant axon. *J Physiol* 239: 393–434, 1974.
- Kuo CC and Bean BP.** Na<sup>+</sup> channels must deactivate to recover from inactivation. *Neuron* 12: 819–829, 1994.
- Laughlin SB and Sejnowski TJ.** Communication in neural networks. *Science* 301: 1870–1874, 2003.
- Levy WB and Baxter RA.** Energy efficient neural codes. *Neural Comput* 8: 531–543, 1996.
- McAllister RE, Noble D, and Tsien RW.** Reconstruction of the electrical activity of cardiac Purkinje fibers. *J Physiol* 251: 1–58, 1975.
- Patlak JB.** Molecular kinetics of voltage-dependent Na<sup>+</sup> channels. *Physiol Rev* 71: 1047–1080, 1991.
- Vandenberg CA and Bezanilla F.** A sodium channel gating model based on single channel, macroscopic ionic and gating currents in the squid giant axon. *Biophys J* 60: 1511–1533, 1991.
- Zagotta WN, Hoshi T, and Aldrich RW.** Shaker potassium channel gating. III. Evaluation of kinetic models for activation. *J Gen Physiol* 103: 321–362, 1994.